JOURNAL OF MATERIALS SCIENCE 24 (1989) 4100–4105

# Diffusion behaviour of the core-sheath structure in E-glass fibres exposed to aqueous HCl

B. D. CADDOCK, K. E. EVANS, I. G. MASTERS*
*Department of Materials Science and Engineering, University of Liverpool, P.O. Box 147, Liverpool L69 3BX, U.K.*

The existence of a characteristic core–sheath morphology in E-glass fibres undergoing acid corrosion is well known. This effect is attributed to the removal of calcium and aluminium ions from the glass structure. Sheath growth measurements indicate that this abstraction involves a two-stage diffusion process, with a room-temperature diffusion coefficient of $1.4 \times 10^{-16}$ m$^2$ sec$^{-1}$ initially, slowing to $1.5 \times 10^{-17}$ m$^2$ sec$^{-1}$ at later times. This two-stage process is related to fibre structure. It is also shown that there is an initial delay, during which the core–sheath structure does not develop.

## 1. Introduction

The nature of the process of corrosion of glass fibres has received a great deal of attention in recent years because of its importance in limiting the performance of glass-fibre reinforced composites. Such composite materials have been known to fail, over a period of years, as a result of a combination of factors including a corrosive environment, temperature and stress [1]. The primary cause of failure is the corrosion and resultant loss of properties of the glass reinforcing fibres.

In the short term, bundle strength is known to depend critically on the flaw distribution in the fibres [2, 3]. In an earlier paper [4] we have shown how this can be characterized by means of the Weibull distribution function. Significant changes in fibre strength were shown to occur following short exposures to aqueous hydrochloric acid. In these short-term tests there was no visible change in the morphology of the fibre cross-sections. In contrast to this, the most characteristic feature of glass fibres undergoing long-term corrosive attack in an acidic environment is the existence of a well-defined core–sheath structure [2]. This outer sheath of material is identifiable both optically, by change of refractive index, and in the scanning electron microscope and grows in size with time on exposure to acid. The mechanical properties of this outer region are considerably reduced, and recent work [3, 4] has shown that the resultant properties of the fibres can be accounted for, to a large extent, by assuming that the mechanical strength of the fibres is wholly due to the central core region. There is, however, considerable doubt [5] as to whether it is this mechanism that is the cause of fibre failure in composites. The existence of a pronounced core–sheath structure in composites is usually the result of post-failure corrosion.

It is possible, however, that core–sheath effects at short times, not previously detected, contribute to failure in the stress–corrosion situation. In order to clarify this area information is required on the rate of core–sheath formation and its relationship to the failure process in the composite. The rate of formation also provides further insight into the chemical processes involved. Originally, the loss of strength of E-glass was believed to be due to the removal of sodium ions [6]. More recently, however, electron microprobe analysis [7] has shown that the predominant structural change under acidic corrosion in the sheath region is the replacement of calcium and aluminium ions by $H^+$ ions. For a fibre immersed in aqueous acid the sheath is believed to consist of demineralized silica that has been hydrated to form a gel [3]. It has been suggested [8] that the ion-exchange process involved in the demineralization is diffusion controlled, either in the glass or the gel phase, and the experiments described below examine this possibility.

## 2. Experimental details

E-glass roving (Equerove 2347, Pilkington Bros. Ltd, Lathom) containing approximately 4000 fibres, of the composition shown in Table I, was used. Sections of fibre 100 mm long were cut, washed in acetone and distilled water, placed in the acid environment and held at a constant 25° C. The acetone wash was used to remove any sizing to ensure free, individual fibres and to ensure that the results obtained measured effects in the glass alone and not the chemical resistance of a particular size. SEM examination (Fig. 1) showed

TABLE I Composition of E-glass (wt %)

| $SiO_2$ | $Al_2O_3$ | CaO | MgO | $Fe_2O_3$ | $Na_2O$ | $K_2O$ | $Ba_2O_3$ |
|---|---|---|---|---|---|---|---|
| 52.4 | 14.9 | 24.0 | 1.8 | 0.4 | 1.0 | 1.0 | 4.3 |

*Present address*: Royal Ordnance Factory, Greater Manchester, UK.



0022–2461/89 $03.00 + .12 

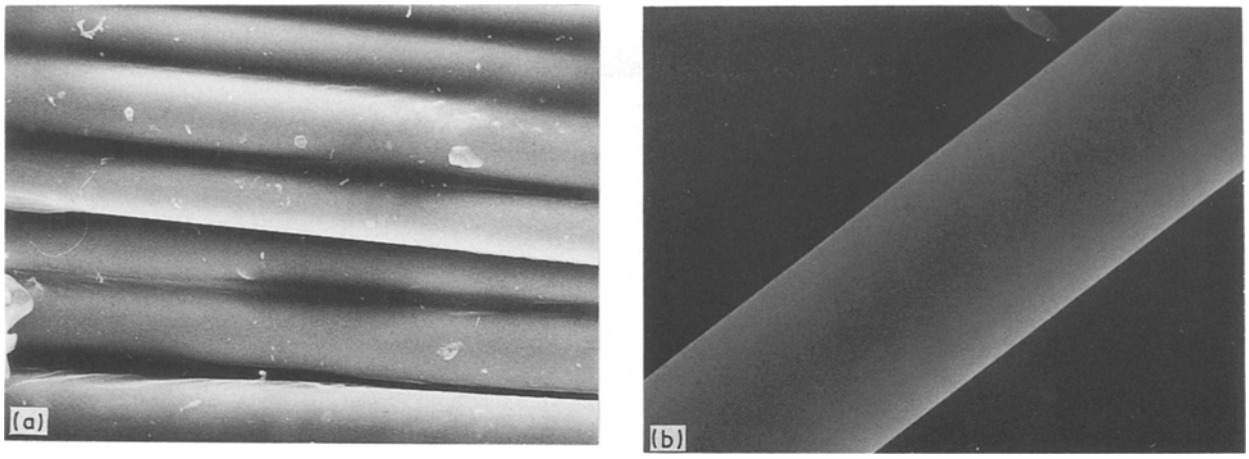


*Figure 1* Scanning electron micrograph of E-glass fibres before and after acetone washing, showing removal of size. (a) Sized fibres, (b) acetone-washed fibre.

that the size was removed by this operation. Specimens were subjected to attack by a range of hydrochloric acid concentrations between 0 and 1 M for times up to 16 d. After testing, specimens were cut and mounted for observation by SEM. Samples were mounted both for observation perpendicular and parallel to the axis. Fig. 2 shows a typical section of fibres that had been exposed to molar acid for 16 h, showing the characteristic core–sheath structure.

Fibre diameters and sheath widths were measured for each sample on up to 200 fibres per sample. A statistical analysis was performed (see Fig. 3 for the unexposed, desized case). The distribution of fibres is slightly skewed, but the overall dependence of both the mean and median diameters and sheath thicknesses varied in very similar ways with concentration and time. In this paper the results represent the mean values.

Energy-dispersive X-ray analysis (EDX) was also performed on a small number of fibres in each specimen, both on the fibre face perpendicular to the axis, and on the fibre surface parallel to the axis. Although this technique is only semi-quantitative, it will be shown below that the peak heights obtained for calcium and aluminium, with respect to the silicon peak as a reference, can be used to obtain information on the rate of diffusion, and agree with other measurements obtained.

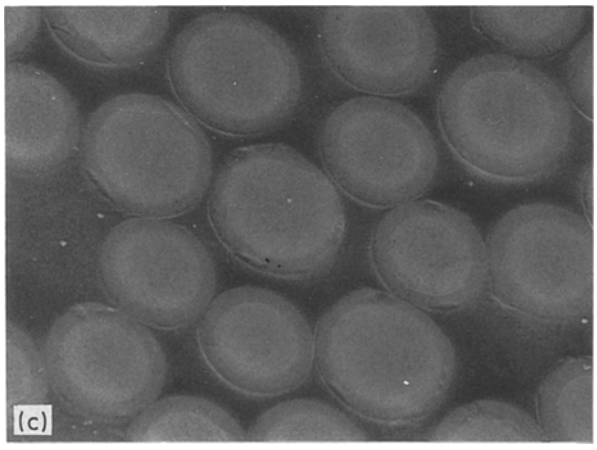


*Figure 2* Scanning electron micrograph of E-glass fibres after 16 h exposure to 1 M HCl, showing characteristic core–sheath structure.

Previous work [3] has shown that the rate of leaching varies through the fibre. It is shown elsewhere [4] that the early phase has important effects on the overall mechanical properties for bundles of glass fibres. It is therefore necessary to measure the rate of leaching from as early as possible, as accurately as possible.

## 3. Results

In all cases, both when visible optically and in the SEM, the overall features of the core–sheath structure are a uniform appearance in the sheath and a sharp boundary between the core and sheath (see Fig. 2). The central region shows a slight variation in intensity. Variation in scanning conditions did not show this to be an artefact of scanning and it may be evidence for density variations across the glass fibre due to cooling rates during manufacture. Such differential cooling rates have been invoked to explain cracking in the sheath region as the mechanical properties degrade [3].

Fig. 4 shows the variation of outer fibre diameter with time for 1 M HCl up to 168 h. At this time the sheath represents more than 50% of the total fibre area. As can be seen, there is no significant change in outer fibre radius. Fig. 5 represents the increase in sheath size as a function of time up to 168 h. Qualitatively, these results are in agreement with similar work on sulphuric acid [3], where it was also shown that the presence of size on the fibre surface had little effect on the overall rate of sheath growth. In Table II the change in sheath size (calculated as an area fraction) is tabulated for three acid concentrations at 16 h.

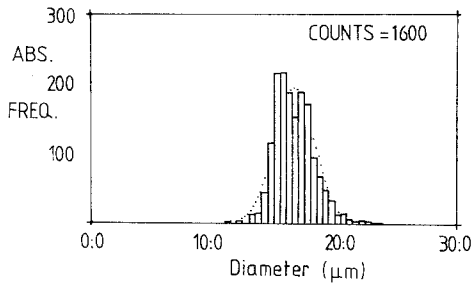


*Figure 3* Statistical analysis of 1600 unexposed fibres, showing distribution of fibre diameters.

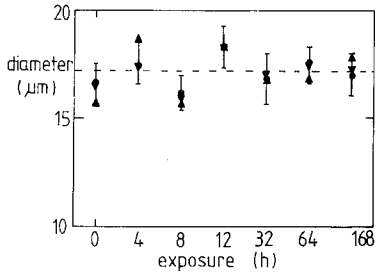


*Figure 4* Variation of outer fibre diameter with duration of exposure to 1 M HCl: (●) mean, (▼) median, (▲) mode.

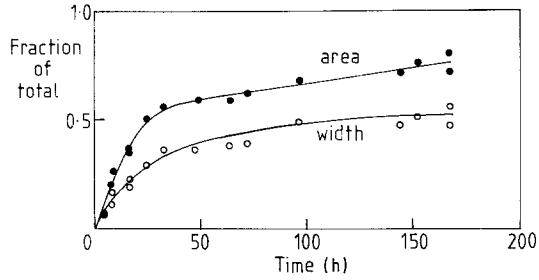


*Figure 5* Variation of fractional sheath width and area plotted as a function of exposure time.

along with peak EDX values. As can be seen, the overall effect is a linear change of sheath width with concentration. This also agrees with previous work relating strength to concentration [8] and strength to residual core diameter [3, 4]. The relationship between mechanical properties and core diameter is explored in detail elsewhere [4].

Fig. 6 shows the variation in peak height for aluminium and calcium, with time, obtained by an EDX analysis from the outer surface of the sheath region in the case of corrosion by 1 M HCl. Although only semi-quantitative, this gives an approximate value for the rate of removal of $Ca^{2+}$ and $Al^{3+}$ ions from the glass. All specimens were mounted on the same SEM stub for the EDX analysis, to ensure maximum quantitative comparability.

A measure of the accuracy of the EDX analysis is obtained by comparing the ratio $SiO_2 : CaO : Al_2O_3$ obtained from the known composition of E-glass to that obtained from the EDX analysis. The known composition ratio is 100:45:29. The experimental value (including a suitable weighting for oxygen) from Table II for the bare fibre is 100:43:32, so that, although only considered to be semi-quantitative, the analysis has an accuracy of about 5 to 10%.

## 4. Analysis of results

From these results it is possible to test whether this process is diffusion dominated and to obtain the appropriate diffusion coefficient. This is done in a number of different ways, each involving some assumptions about the process, but which should lead to a consistent value if the leaching mechanism follows a simple diffusion law. The various diffusion coefficient estimates were made as follows.

1. From the observation of a sharp core–sheath interface and from the EDX analysis, the problem is seen to be one of a moving boundary. The simplest interpretation is to assume that calcium and aluminium are leached out from the glass surface at the core–sheath interface (presumably by $H^+$ ion replacement from the HCl) with very little diffusion occurring in the bulk of the glass (i.e. a low diffusion coefficient). A similar approach has been used with some success to explain sodium depletion in sodium-rich glass corrosion [9–11]. In the present work the interest is not so much in the mechanism of ion exchange, but in obtaining quantitative estimates for the rate of diffusion. The simplest approximation is to assume that we have moving boundary diffusion, in which case

$$D \simeq r^2/t \tag{1}$$

where $r$ is the width of the sheath, increasing with time $t$. This equation will break down as $r$ approaches the radius of the fibre, where the assumption of simple planar diffusion fails. Such an expression can be shown to be exact [12] for the specific case of a semi-infinite medium, where

$$C/C_0 = \text{erfc}\,[x/2(Dt)^{1/2}] \tag{2}$$

in which $C$ is the concentration of diffusant at time $t$ at a depth $x$ below the surface of a plate specimen, and $C_0$ is the surface concentration of diffusant at saturation. If we assume that the observed moving boundary is equivalent to a specific concentration of diffusant, say $C = 0.5C_0$, then

$$x/2(Dt)^{1/2} = 0.4795 \tag{3}$$

hence

$$D \simeq x^2/t \tag{4}$$

For more complex geometries the same expression results, but with different front factors.

In Fig. 7, $r$ is plotted against $t^{1/2}$. As can be seen, the variation is clearly not linear. The results, however, can be interpreted in terms of a short-time and a long-time diffusion coefficient. By taking the gradients of the two lines in Fig. 7 it can be seen that at early

TABLE II Sheath width and EDAX counts (reference is Si = 100) as a function of HCl concentration. Exposure = 16 h

| Concentrated M | Fractional sheath width | EDX count | | | | Unexposed | |
|---|---|---|---|---|---|---|---|
| | | Core | | Sheath | | Ca | Al |
| | | Ca | Al | Ca | Al | | |
| 1.0 | 0.24 | 63 | 29 | 17 | 9 | 66 | 32 |
| | | ±3 | ±1 | ±6 | ±1 | ±3 | ±2 |
| 0.8 | 0.18 | 62 | 30 | 22 | 11 | | |
| | | ±3 | ±1 | ±10 | ±3 | | |
| 0.6 | 0.12 | 63 | 28 | 24 | 12 | | |
| | | ±3 | ±1 | ±6 | ±3 | | |

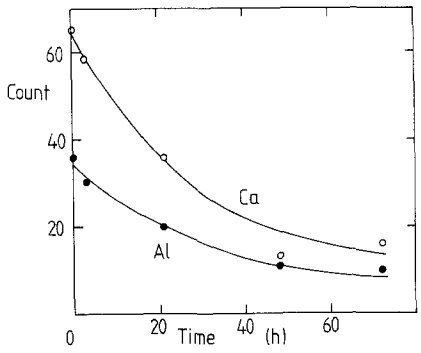


*Figure 6* EDX peak counts in sheath region for aluminium and calcium, taken on the surface parallel to the fibre axis, as a function of exposure time.

times the diffusion coefficient, $D_1$, is approximately $1.4 \times 10^{-16}\,m^2\,sec^{-1}$, falling to $D_2 = 1.5 \times 10^{-17}\,m^2\,sec^{-1}$ at longer times.

2. For short times, a more accurate approach is to use the solution for diffusion in a cylinder [12], by assuming that the area of the sheath represents an area of total depletion and the area of the core an area of negligible depletion. Then the fraction depleted at time $t$, $M_t/M_\infty$, can be used to obtain the diffusion coefficient from the equation given in [12]

$$M_t/M_\infty = 4(Dt)^{1/2}/(\pi)^{1/2}a \qquad (5)$$

so a plot of $M_t/M_\infty$ against $t^{1/2}$ should be linear for simple diffusion. Such a plot is given in Fig. 8. This plot gives an initial value of $D_1 \simeq 7.4 \times 10^{-17}\,m^2\,sec^{-1}$, which is reasonably close to the estimates quoted above. For longer times, Equation 5 breaks down.

While the method based on Equation 1 is less accurate at short times than that based on Equation 5, it has the advantage of remaining valid (i.e. $D \propto t$) for all times. Another key feature to note in Figs 7 and 8 is that the diffusion process does not appear to start until after about 2 to 3 h at this temperature.

Finally, to illustrate the deviation in behaviour from a simple diffusion process, involving a single constant diffusion coefficient, we can calculate $D$ from a plot of $M_t/M_\infty$ against time, as opposed to $t^{1/2}$. This treatment follows that developed by Ellis and Found [13], who showed that, for a thin flat plate, the time required for $M_t/M_\infty = 0.5$, designated $t_{1/2}$, is related to the plate thickness, $T$, and the diffusion coefficient by the simple equation

$$D = 0.049T^2/t_{1/2} \qquad (6)$$

It has been shown [14] that a similar equation can be

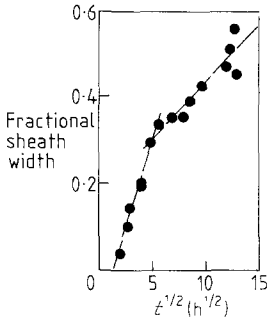


*Figure 7* Fractional sheath width plotted against $t^{1/2}$.

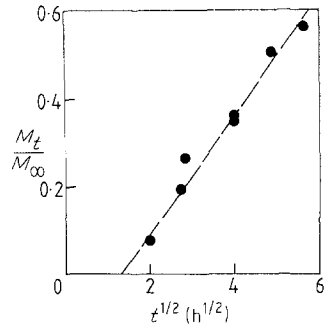


*Figure 8* $M_t/M$ plotted against $t^{1/2}$.

derived for a cylinder of radius $a$ such that

$$D = 0.063a^2/t_{1/2} \qquad (7)$$

The required plot of $M_t/M_\infty$ against time is shown in Fig. 9, from which Equation 7 gives $D = 5.0 \times 10^{-17}\,m^2\,sec^{-1}$, lying between the two previous estimates. We can use this single value to plot the full change in the variation of fractional sheath area with time, and this profile is also shown in Fig. 9. As can be seen, this model of simple diffusion underestimates $D$ initially and overestimates it at longer times.

It is also of interest to consider the relative rates at which calcium and aluminium are leached out of the surface layers of the glass. This is shown by the data in Fig. 6, from which it can be seen that the depletion rates for calcium and aluminium are very similar, with the diffusion of calcium out of the glass being possibly slightly faster than that of aluminium.

From the results of Table II we have that the sheath width is a function of acid concentration (i.e. $H^+$ concentration). The EDX peaks show a small change with acid concentration, but this is believed to be due to the lack of resolution of the EDX analysis ($\simeq 1\,\mu m$) and that within the experimental error of the measurements the calcium and aluminium concentrations are approximately constant in the depleted sheath.

## 5. Discussion

From the results above it is obvious that core–sheath growth is not a simple Fickian diffusion process. From Figs 8 and 9 it is seen that the process is characterized by a varying effective diffusion coefficient and that the process does not begin at time zero. Two explanations are available which can account for the first of these phenomena. Firstly that the glass structure varies with radius and hence the rate of diffusion changes [3]. Secondly that the diffusion process is concentration

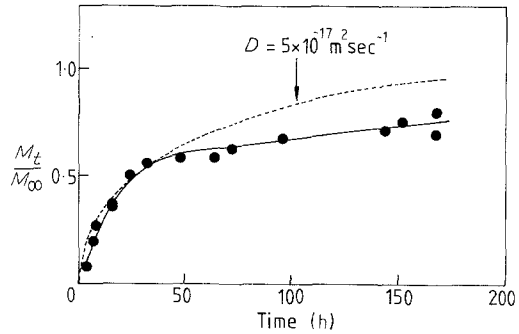


*Figure 9* $M_t/M$ plotted against $t$.

dependent. This latter possibility has been considered in detail [9–11] for the case of sodium removal from soda-lime glass. The mathematical description given in these earlier papers provides an explanation for the steep concentration gradients observed both with soda-lime glass and in our work with E-glass fibres. Applying the same approach here, we may, to a first approximation, describe the process by an effective diffusion coefficient, $D_{\text{eff}}$, given by

$$D_{\text{eff}} = D_{\text{Ca}} D_{\text{H}} / [C_{\text{Ca}} D_{\text{Ca}} + C_{\text{H}} D_{\text{H}}] \quad (8)$$

where $D_{\text{Ca}}$ and $D_{\text{H}}$ are the diffusion coefficients of $Ca^{2+}$ and $H^+$ ions in the glass and $C_{\text{Ca}}$ and $C_{\text{H}}$ their fractional concentrations. At short times the diffusion of $H^+$ ions into the glass is fed by the concentration of $H^+$ ions in the acid, which, because of the high acid molarity, is much higher than the $Ca^{2+}$ concentration in the glass surface. Hence at short times in Equation 8 $C_{\text{H}} \gg C_{\text{Ca}}$ so $D_{\text{eff}} \simeq D_{\text{Ca}}$. At later times, $D_{\text{eff}}$ is seen to fall by an order of magnitude. Again, Equation 8 asserts that even when $C_{\text{H}} \simeq C_{\text{Ca}}$, $D_{\text{eff}}$ will be dominated by $D_{\text{H}}$.

Thus, $D_1 \simeq D_{\text{Ca}}$ and $D_2 \simeq D_{\text{H}}$. This is in agreement with the work of Doremus and co-workers [10, 11] where the diffusion coefficient for sodium ions was also shown to be much greater than the effective diffusion coefficient for hydrogen ions in soda-lime glass. A further argument to support $D_{\text{Ca}} \gg D_{\text{H}}$ is simply the fact that the sheath is seen to be totally depleted of calcium [14] at all times, even from the earliest development of the sheath region. This shows that the calcium ions are extemely mobile in the glass under these conditions. In sheath development at longer times, therefore, the limiting step is the rate of ingress of hydrogen ions to replace the calcium. It is considered, however, that although this explanation is reasonable, the alternative of variable glass structure cannot be discounted.

The apparent delay in the commencement of the diffusion process could be explained by assuming that a residue from the fibre size is still present on the fibre surface. Although acetone washing will remove the organic material from the fibres, it may still leave a silica-rich (and hence calcium- and aluminium-depleted) region around the fibre. This would impede the commencement of the acid attack. It is interesting to note that the existence of this zero-time effect coincides with a statistical variation in failure strengths of glass bundles [4], confirming that this is indeed a real effect. This short time period (2 to 3 h) is characterized by a large increase in the Weibull scale parameter for a bundle of fibres, followed at later times by a monotonic fall. The fact that the core–sheath formation process has such a zero time offset indicates that it has no role to play in the failure of glass fibres in stress-corroded composites. This has been borne out by detailed TEM analysis of fibre surfaces that have fractured as a consequence of stress corrosion [14]. Gross depletion of calcium or aluminium does not occur within the timescale for fibre fracture, down to a resolution of 0.1 $\mu$m, for fibres failing under a combination of stress and acid attack. It is conjectured that it is the initial demineralization of the glass surface that is the key process in the stress–corrosion mechanism, rather than the much more extensive effects associated with the growth of a visible sheath.

Additional support for this view is obtained from a study of the data in Fig. 4. This shows the variation in the outer diameter of fibres exhibiting a range of sheath development. As can be seen there is no evidence of a difference in outer diameter for fresh fibres compared with severely corroded fibres. The data all relate to fibres in the dried condition. This finding is in accord with the observation [3, 7] that the spontaneous cracking of fibres following fibre ageing in relatively strong acid is caused by the development of differential shrinkage stresses only during the drying of the hydrated silica sheath and not in the wet state.

It is suggested, therefore, that spontaneous fibre cracking without applied stress is exclusively a feature of fibre ageing and core–sheath development. The conditions necessary for the development of shrinkage stresses resulting from sheath dehydration are unlikely to occur during stress-activated corrosion, because the process occurs in a predominantly wet, rather than a drying situation.

## 6. Conclusions

The core–sheath process in glass fibres is a complex diffusion process, characterized by a varying diffusion coefficient, which results either from a concentration-dependent diffusion process or from structural variations in the glass. The process is also characterized by an initial delay for periods of 2 to 3 h at room temperature before measurable core–sheath growth begins. Again, this effect may be the result of variations in the glass structure at the fibre surface. It is considered that the development of the core–sheath morphology is exclusively a feature of fibre ageing. The stress-activated fracture of glass fibres in aqueous environments occurs over too short a timescale for a properly defined sheath to develop. The stress-corrosion process in glass fibre composites is therefore believed to involve a much less extensive form of fibre-surface demineralization.

## Acknowledgement

The authors thank Professor D. Hull, University of Cambridge, for many stimulating discussions in this area of work.

## References

1. P. J. HOGG and D. HULL, in "Developments in GRP Technology – 1", edited by B. Harris (Applied Science, London, 1983) p. 37.
2. A. G. METCALFE, M. E. GULDEN and G. K. SCHMITZ, *Glass Technol.* **12** (1971) 15.
3. A. BLEDSKI, R. SPAUDE and G. W. EHRENSTEIN, *Comp. Sci. Technol.* **23** (1985) 263.
4. K. E. EVANS, B. D. CADDOCK and K. L. AINSWORTH, *J. Mater. Sci.* **23** (1988) 2926.
5. J. N. PRICE and D. HULL, *ibid.* **18** (1983) 2798.
6. A. G. METCALFE and G. K. SCHMITZ, *Glass Technol.* **13** (1972) 5.
7. H. A. BARKER, I. G. BAIRD-SMITH and F. R. JONES, Paper 12, Symposium on Reinforced Plastics in Anticorrosion Applications, NEL, East Kilbride, 1979 (NEL, East Kilbride, Glasgow, 1979).

8. H. D. CHANDLER and R. L. JONES, *J. Mater. Sci.* **19** (1979) 3849.
9. B. M. J. SMETS and M. G. W. THOLEN, *J. Amer. Ceram. Soc.* **67** (1984) 281.
10. R. H. DOREMUS, Y. MEHROTA, W. A. LANFORD and C. BURMAN, *J. Mater. Sci.* **18** (1983) 612.
11. W. A. LANFORD, K. DAVIS, P. LAMARCHE, T. LAURSEN, R. GROLEAU and R. H. DOREMUS, *J. Non-Cryst. Solids* **33** (1979) 249.
12. J. CRANK, "The Mathematics of Diffusion" (Oxford University Press, 1985).
13. B. ELLIS and M. S. FOUND, *Composites* **14**(3) (1983) 237.
14. B. D. CADDOCK, PhD thesis, University of Liverpool, October 1987.

*Received 21 October 1988*
*and accepted 22 February 1989*